EFFECTS OF CARBON DIOXIDE INJECTION ON SCALING

A. T. Bogorosh, I. M. Fedotkin,
I. S. Gulyi, and N. I. Oseiko

UDC 664.1:621.565.94.015.24

An effective method has been devised for preventing scaling in heat exchangers; a mathematical model is presented for the scale formation.

Most heat exchangers employ water containing a certain hardness as the heat carrier, and consequently scale is formed on the heat-transfer surfaces, which causes additional fuel wastage and other undesirable effects. It is therefore very important to combat scaling in heat exchangers. Although there have been many studies of scaling, there is as yet no agreed view on the mechanism; various results [20, 21, 24, 32, 33, 35, 44, 45, 48] indicate that the various salts present in the water form scales of various chemical compositions and mechanical properties. It has been shown [24] that the scale structure is dependent on the point where most of the salt crystallizes (on the heating surface or within the liquid), and also on the properties of the salt itself. The rate of scale crystallization is dependent on the temperature of the solution and the concentration of the corresponding ions, i.e., the overall concentration. A decisive effect on the scaling rate comes from the component first deposited in the solid: calcium sulfate or carbonate. In the first case, one gets a gypsum scale, and in the second, a carbonate one. No explanation has yet been published for this. Our views on scaling have been built up in the main from two papers [46, 47]. Additions to the data are also to be found in [32, 21, 33]. At the present time, scaling is considered not as a cyclic deposition of the entire dry matter from the solution on bubble formation [46], nor as due to electrical disequilibrium at the surfaces [45], which may have local positive and negative charges, but instead as a complex electromechanical crystallization involving various physicochemical and thermomechanical factors [7, 40, 41].

The thermal resistance of scale is dependent on various factors, including the salt composition of the water, the ionic combustion of the salts, the salt concentrations in the working solution, the heat loading on the surface, the temperature of the working liquid, the detailed heating process (usually single-phase or two-phase gas–liquid type), the liquid–gas relation, and other effects of hydrodynamic and heat-transfer types. These factors determine the composition and structure of the scale, the scaling rate, and the increment in the thermal resistance of the scale. We therefore have to consider how to calculate the major characteristics and parameters of the process, which varies over a certain time interval, although so far there has been no agreed view on the various aspects.

Some methods of combatting scaling are advantageous on model solutions and on laboratory equipment; however, the results have not been reproduced on actual plant. We consider this as being due to the complex process being at present difficult or impossible to simulate. It is therefore necessary to examine the scaling directly under industrial conditions on actual plant.

Most methods of combatting scaling are of particular character and are applicable only in particular cases; reagent-free methods appear advantageous, but the need for constant flushing reduces the performance of the electromagnetic method [1, 4-6, 12-29, 31, 34, 36, 37, 43], and also of the acoustic [2, 30], hydromechanical, and other methods. These techniques are applicable in heat-transfer flow systems and certain types of steam boilers. In other areas of engineering, such as chemical engineering, food engineering, desalination, and so on, such methods are not always applicable on account of their adverse effects on the quality of the final product. We have examined the effects of flushing with industrial saturation gas on

---

Kiev Institute of Food-Industry Technology. Translated from Inzhenerno-Fizicheskii Zhurnal, Vol. 28, No. 4, pp. 723-734, April, 1975. Original article submitted July 11, 1973.

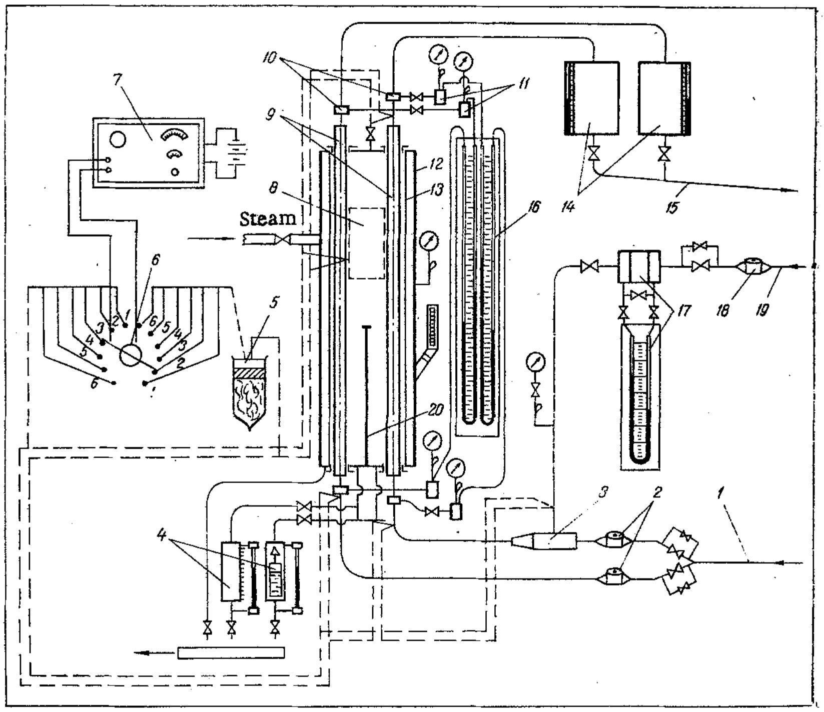

Fig. 1. The apparatus: 1) solution feed pipe; 2) accumulating flowmeters; 3) gas–liquid mixer; 4) condensate meters; 5) Dewar vessel; 6) thermocouple switch; 7) UPIP-63M potentiometer; 8) steam inlet; 9) trial tubes; 10) pressurized samplers; 11) dampers; 12) body of heat exchanger;. 13) internal jacket to eliminate condensate from outer jacket; 14) metering tanks; 15) solution takeoff to plant; 16) differential pressure gauges; 17) gas flowmeter with double diaphragms and U-tube manometer; 18) accumulating gas flowmeter; 19) gas from plant; 20) baffle between trial tubes.

the scaling during heating of sugar solutions of concentrations up to 15 % which contain numerous inorganic and organic salts.

We use the method of [3] to record the major technological and other characteristics of the sealing in the heat-transfer equipment and circulation loops containing one-phase and two-phase gas–liquid mixtures.

Figure 1 shows the apparatus for examining the scaling in these heat exchangers; this could be used directly in actual plants with heat-transfer tubes of diameter 33/30, length 1500 mm, and made of brass, stainless steel, or ordinary steel. The tubes were removed after each series of tests and cut open along the length to measure the scale thickness and to take samples for physicochemical examination.

The tests were done with sugar solution and technological water of total hardness 13°H at heat loadings from 0.00006 to 0.6 MW/m^2. The reduced liquid flow rates varied from 0.2 to 2.5 m/sec, and the gas ones from 0.2 to 10 m/sec, the parameters of the saturated steam varying from 0.2 to 5 atm.

Figure 2 shows the variation in scale thickness along a heat-transfer tube with the one-phase and two-phase heating methods for the technical water after 250 h; the scale thickness is clearly much less in the two-phase gas–liquid mode.

Figure 3 shows that the thermal conductivity of the scale as a function of thickness is represented by a straight line in logarithmic coordinates. The maximum scale thickness was 0.15 mm for the two-phase case (lines 1 and 3 of Fig. 3); here the $\lambda_s = f(\delta_s)$ curves are represented by the empirical formulas

$$\lg \lambda_s = a + b \lg \delta_s, \ \frac{\mathrm{W}}{\mathrm{m \cdot deg}}, \tag{1}$$

$$\lambda_s = 10^a \delta_s^b, \ \frac{\mathrm{W}}{\mathrm{m \cdot deg}}, \tag{2}$$

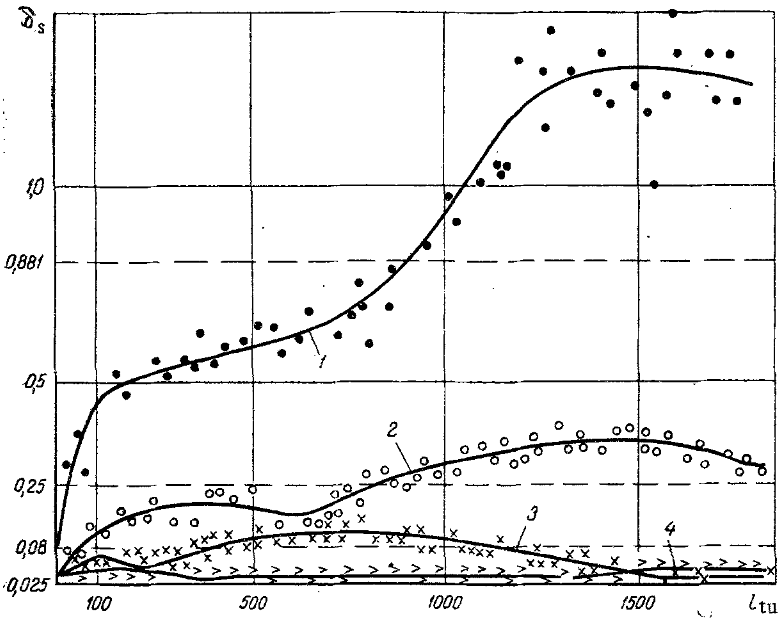

Fig. 2. Variation in scale thickness along tubes (heating zone from 0 to 1500 mm): 1) after 250 h with a solution containing 2.5 %CaO; 2) after 120 h with a solution free from CaO (curves 1 and 2 are for the normal working state); 3) after 250 h with a solution containing 2.5 % CaO; 4) after 120 h with a solution free from CaO (curves 3 and 4 are for the two-phase state); δ_s in mm, l_{tu} in mm.

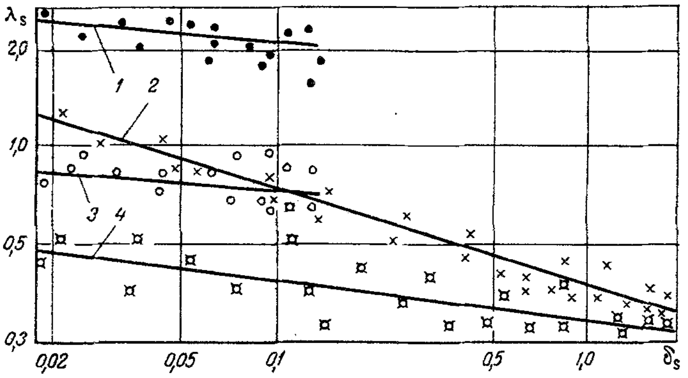

Fig. 3. Thermal conductivity of scale as a function of thickness: 1 and 3) two-phase heating; 2 and 4) ordinary heating; flow speeds, m/sec: 1 and 2) 1.5; 3 and 4) 0.5; λ_s in W/m · °C.

which apply for two-phase heat transfers for $\delta_s \leq 0.15$ mm; Table 1 gives the values of the constants *a* and b in (1) and (2).

The thermal scaling coefficient ψ was calculated from the formula of [38] and varied less in the two-phase equipments than it did in the one-phase ones (Fig. 4).

The definition of ψ indicates that the thermal resistance of the scale R_s can be represented for these two cases as

$$R_{s_1} = \psi_1 q\tau, \text{m} \cdot \text{deg/W}, \tag{3}$$

$$R_{s_2} = \psi_2 q\tau, \text{m} \cdot \text{deg/W}. \tag{3a}$$

TABLE 1. Values of *a* and b in (1) and (2)

Reduced flow speed	Single-phase heating (lines 2 and 4)		Two-phase heating (lines 1 and 3)	
	a	b	a	b
0,5	$10^{-0,554}$	—0,278	$10^{-1,1967}$	—0,06634
1,5	$10^{-1,562}$	—0,4027	$10^{-0,7013}$	—0,05819

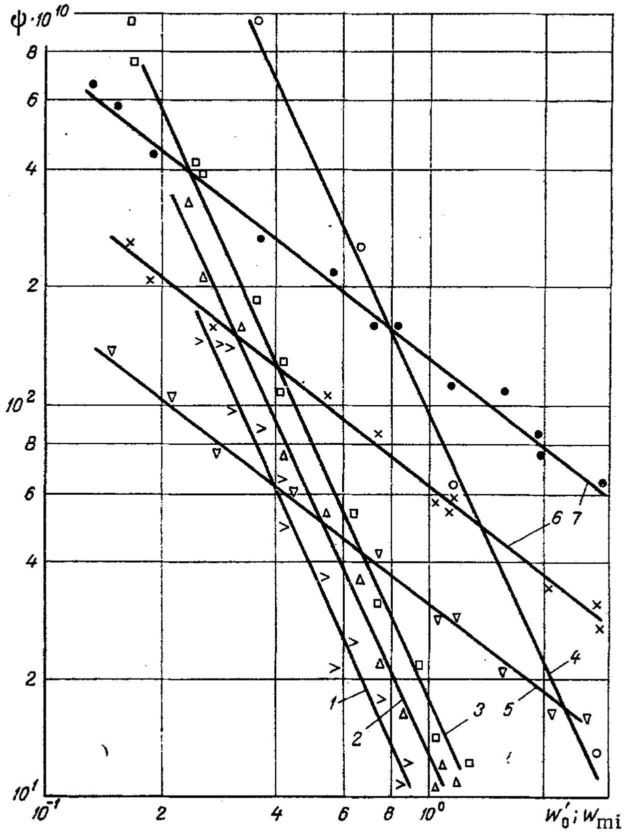

Fig. 4. Temperature coefficient of scaling as a function of flow speed: 1) with 2.5 %CaO; 2) without CaO; 3) technical water; 4) data of [38]; 5) with 2.5 %CaO; 6) without CaO; 7) technical water (curves 5-7 are for two-phase heating).

Figure 4 shows that the power n in the formula of [38] differs from our results (lines 5-7), and

$$\psi_1 = C \cdot 10^{-10} W_0'^{\,-n}, \tag{4}$$

$$\psi_2 = C \cdot 10^{-10} (W_0' + W_0'')^{-n}. \tag{4a}$$

We derived a relationship for the optimal mode of operation of a two-phase exchanger:

$$K = ab^{G_g} \cdot 10^2, \text{ W/m}^2. \tag{5}$$

Table 2 gives the value for *a* and b in relation to the working time for a technical solution with contents of 12-15% dry material without CaO and with the addition of 2.5 %CaO in accordance with the technique appropriate to dry-matter contents of 12-15 %.

The values in Tables 1 and 2 show that the amount of injected gas must be reduced as time passes when the solution contains 2.5% CaO, while no such restriction is required for the CaO-free case.

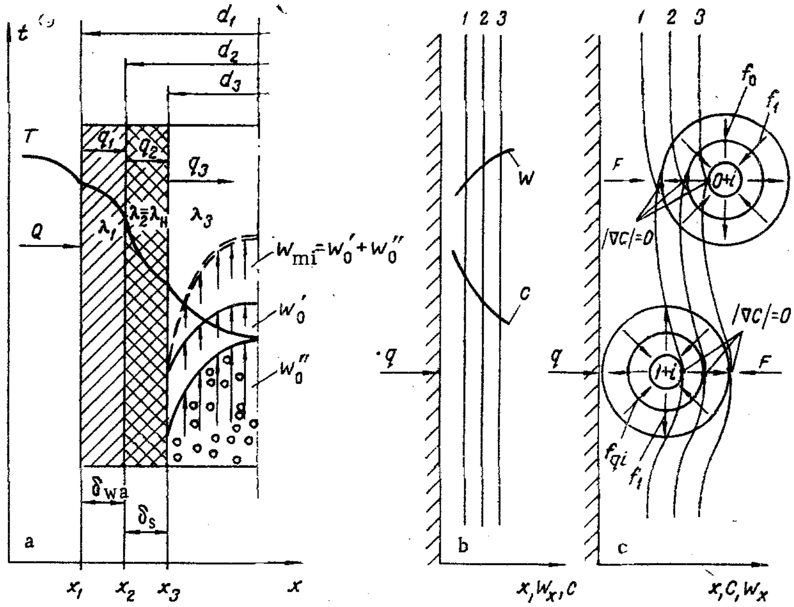

Fig. 5. Theoretical model: a) temperature distributions in one-phase and two-phase heating; b) parallel velocity sections of one-phase flow in boundary layer; c) flowline perturbations due to turbulent pulsations produced by gas injection: 1) $C_1 = 1.0$; 2) 0.5; 3) 0; t, °C.

TABLE 2. Values of *a* and b for (5)

Op.time, h	Values		Op.time, h	Values	
	a	b		a	b
No CaO			+ *2.5%* CaO		
			30	0,37	6,7
< 30	0.2	8	50	0,4	8,0
80	0.1	10	80	0,35	9,0
100	0.374	7	100	0,35	10,0
120	0.1	9	150	0,4	12,0
			200	0,4	15
			≥ 250	0,4	18

Physicochemical methods [40] gave the chemical and phase compositions of the scale on heating solutions for 250 h in actual working conditions with various working parameters.

The thermochemical transformation products from the organic substances affect the color of the scale, the strength of the structure, and the rate of formation of crystallization centers in the layer near the wall. The amount of these products in the scale from a two-phase exchanger (Table 3) was less by a factor 3 than that in an ordinary one-phase one; the organic materials are firmly bound to the inorganic part of the scale and substantially influence the deposition rate and scale composition.

The results give a first indication of the scale formation mechanism with gas injection.

Crystallization centers are produced at the heating surface if the scaling solution becomes supersaturated there, which can occur on account of evaporation in the microzone. The effect can be reduced by depressing the adhesion of the deposit, displacing the crystallization zone from the boundary layer to the bulk solution, or causing the material to deposit in the solid state outside the heating zone.

In a two-phase flow, crystallization is accelerated by the bubbles of gas in the solution [7], the energy of nucleation at the gas–bubble surfaces will be less than that at the heating surface, so most of the deposition occurs at the solution–gas boundary.

TABLE 3. Chemical and Phase Compositions (%) for Scale in Single-Phase and Two-Phase Heat Exchangers

Composition characteristic	Single-phase	Two-phase
Free Water;*	2,58—3,94	0,51—1,26
Firing loss	46,23—52,62	43,89—46,45
Ash	47,38—53,77	53,55—56,11
Organic matter	13	4,5
Including scale extract	8,6	3,4
Unextracted fraction	4,4	1,1
Calcium oxide	32,8—35,36	33,8—39,95
Calcium	23,49—26,3	24,18—28,08
Magnesium oxide	4,01—4,49	2,67—3,03
Magnesium	2,42—2,71	1,0—1,83
Silicon dioxide	2,29—2,57	0,62—0,87
Iron oxide	0,76—1,06	1,25—2,02
Iron	0,53—0,74	0,5—0,71
Aluminum oxide	0,13—0,15	0,37—0,41
Aluminum	0,07—0,08	0,1—0,11
Sodium	0,37—0,48	0,3—0,41
Lead	0,05	0,05
Manganese	0,1	0,1
Phosphorus and barium	Not obs.	
Phase composition of components:		
calcium carbonate	58,5—63,0	60,2—71,0
xonotlite	0,6—0,9	0,1—0,2
gypsum	0,1	0,1—0,4
magnesium carbonate	4,63—5,15	5,9—5,73
brucite	0,14—0,28	0,08—0,12
serpentite	3,75—4,15	0 41—0,73
kaolinite	0,11	0,27
pyrophyllite	0,27—0,34	0,50—0,64
analcime	0,4	0,1
hematite	0,1	0,2
magnetite	0,1	0,3
phosphorite	None	up to 0,7
siderite	0,2	0,4—1,2
natrolite	0,1	0,1—0,2
hydrargillite	0,5	0,2
calcium oxalate	0,1	0,05
calcium pectinate	0,2	traces

---

*Scale specimens subsequently analyzed after drying at 100°C.

Figure 5 shows the temperature distribution in a working tube; Figure 5a shows the velocity distribution in the boundary layer for one-phase laminar flow. The concentrations of scale-forming products in the solution increase as the flow speed in the boundary layer is reduced (Fig. 5b). Figure 5c shows the effects of turbulence produced by injecting gas; the speed of the mixture in that case is

$$W_{\text{mi}} = W'_0 + W''_0, \text{ m/sec.} \tag{6}$$

The arrows F in Fig. 5 show the vertical turbulent pulsations in the carrying liquid, which increase on injecting gas; this is confirmed by a standard equation [7] derived from the relationship for the total kinetic energy of a multicomponent system:

$$\langle U'^2_{3_l} \rangle = \frac{P_{\text{sf}} - \rho_g S_g \langle U'^2_{3_g} \rangle - \int\limits_0^{x_3} (\rho_g S_g + \rho_l S_l) g dx_3}{\rho_l (1 - S_g)}. \tag{7}$$

We see from (7) that the second and third terms in the numerator are very small, and if we neglect them on the assumption that $S_g = 0.5$, the denominator will be half the numerator, i.e., the mixing in the boundary layer will be doubled in rate, which accelerates the heat transfer, reduces the nucleation rate in the cells in the turbulent jets, and causes more rapid heat transfer to the core of the flow, as is clear from the energy equation [8-11]:

$$\langle U'^2 \rangle = \int\limits_0^{\infty} E(\omega) \cos \omega d\omega. \tag{8}$$

The kinetic equation for heat transport from the wall to the turbulent core can be put as

$$\frac{\omega\nu}{v_*^2}\,\frac{\partial T}{\partial \tilde{t}} + \tilde{v}_k\,\frac{\partial T}{\partial \tilde{x}_k} = \mathrm{Pr}\,\nabla^2 T + \sum_0^i q_i, \tag{9}$$

where $\tilde{v}_k = v_k/v_*$ along the X_k axis (dimensionless), $v_* = \sqrt{\tau_0/\rho}$ is the dynamic velocity, and $\tilde{t} = t/T$; $\tilde{x}_k = X_k v_*/\nu = \mathrm{Re}_k(X_k)$; $\omega = 2\pi/T_n$, cm^{-1}.

By analogy with the heat-balance Eq. (9) we can write the mass-transport equation for the direction from flow to the wall or vice versa as

$$\frac{\omega\nu}{v^2}\,\frac{\partial C}{\partial \tilde{t}} + \tilde{v}\,\frac{\partial C}{\partial \tilde{x}_k} = S\nabla^2 C + \Theta, \tag{10}$$

where $S = \nu^D/\nu$.

The term $\sum_0^i q_i$ in (9) most characteristic of our case is of interest from the viewpoint of q, the flux of material to the heat-transfer surface or vice versa, i.e.,

$$q_{\mathrm{wa}} = \frac{\nabla^2 C}{|\nabla C|}\,\frac{\nabla C}{|\nabla C|}, \tag{11}$$

where $|\Delta C|$ represents the modulus and ∇^2 is the Laplace operator; if $|\nabla C| = 0$ (Fig. 5) at the nodes where the derivative is zero, we have

$$q_{\mathrm{wa}} \to \infty. \tag{11a}$$

Analysis of (7)-(11) indicates that the scaling will always be less in a two-phase flow on account of the mixing of the liquid by the gas, as (7) shows, and also because of the more rapid heat transfer to the core of the flow, as (8), (9), and (11) show.

In the general case, the rate of growth of the scale on the heat-transfer surface can be represented as

$$R_s = \frac{\delta_s(\tau)}{\lambda_s(\tau)} = \frac{1}{K} = \frac{F_S \Delta t}{Q}, \tag{12}$$

where

$$\frac{dR_s}{d\tau} = \frac{\lambda_s \dfrac{d\delta_s}{d\tau} - \delta_s \dfrac{d\lambda_s}{d\tau}}{\lambda_s^2}, \tag{13}$$

or

$$\frac{dR_s}{d\tau} = \frac{QF_S \dfrac{d\Delta t}{d\tau} - F_S \Delta t \dfrac{dQ}{d\tau}}{Q^2}. \tag{14}$$

Similarly, we get the equation for the increase in scale thickness on the heating surface:

$$\frac{d\delta_s}{d\tau} = \lambda_s \frac{dR_s}{d\tau} + \delta_s \frac{d\ln\lambda_s}{d\tau}, \tag{15}$$

then with (14) we have

$$\frac{d\delta_s}{d\tau} = \lambda_s \frac{F_S \dfrac{d\Delta t}{d\tau}}{Q} - \lambda_s \frac{F_S \Delta t \dfrac{dQ}{d\tau}}{Q^2} + \delta_s \frac{d\ln\lambda_s}{d\tau}. \tag{16}$$

The following is the final form for the relation between δ_S and τ:

$$\tau = \frac{(q_4 + q_2 + q_{\mathrm{wa}})\,q_3}{q_1^2} \ln \frac{q_3 - b'q_1}{(q_3 - b' + \delta_s)\,q_1} - \frac{q_4 + q_2 + q_{\mathrm{wa}}}{q_1} + \frac{q_2 b'}{q_3} \ln \frac{1 - \dfrac{q_1\delta_s}{q_3 - b'q_1}}{1 - \dfrac{b'}{\delta_{\text{н}}}}. \tag{17}$$

It follows from (16) and (17) that the rate of scale growth is related to the rate of change in the heat flux, solution speed, temperature difference, thermal conductivities of the media, gas content of the flow, and so on; we have therefore checked (17) by experiment and found good agreement.

Theoretical analysis and experiments on gas injection in scaling thus indicate that the method has practical advantages for heating technical solutions.

The tests show that only about 1.0 m^3/h of gas is needed per 100 m^2 of heating surface in order to reduce the scale thickness by more than a factor of 10; the introduction of the gas–liquid heating scheme for multicomponent technical solutions at one of the plants will give an average saving of 50,000 rubles per year [7]. It is therefore necessary to perform the appropriate studies on heat transfer in gas–liquid conditions as applied in other branches of engineering where scaling is important.

This gas–liquid heating method for reducing scaling should thus find a general use in many branches of engineering.

NOTATION

W_{mi}	is the mixture velocity;
W_0'	is the reduced liquid velocity;
W_0''	is the reduced gas velocity;
Δp	is the pressure drop at entrance and exit of heat-transfer tubes;
K	is the heat-transfer coefficient;
Δt	is the available mean logarithmic temperature difference;
λ_s	is the thermal conductivity of scale;
S_s	is the growth rate on the wall;
δ_s	is the scale thickness;
ψ	is the temperature coefficient of scale formation;
q	is the heat flux;
R_s	is the thermal resistance of scale;
τ	is the time, h;
G_g	is the amount of injected gas;
C_1, C_2, C_3	are the concentrations of scale-forming salts in boundary layers;
$< V'^2_{3l} >$	are the vertical turbulent pulsations of working fluid;
$< V'^2_{3g} >$	is the pulsational velocity of gas in tube;
P_{sf}	is the stagnant-flow pressure constant;
S_g	is the volume gas content;
D	is the diffusion coefficient;
ρ_g, ρ_l	are the gas and liquid densities;
τ_0	is the wall friction;
$E(\omega)$	is the specific energy of turbulent pulsations;
ω	is the characteristic frequency;
T, t	are the temperatures;
T_p	is the characteristic time of process;
F	is the turbulent pulsation force;
f_0, f_1, f_{q_i}	are the elementary diffusion and thermal forces;
F_S	is the surface heating area;
Q	is the total heat flux;
a, b, n	are the constants;
Θ	is the distribution of sink intensity;
S	is the criterial Schmidt number;
$\lvert\Delta C\rvert$	is the concentration modulus at nodes;
∇^2	is the Laplacian;
$q_1 = \alpha_{pi}(t_{wa} - t_{cr}) = G_c\gamma_c r / F_S\tau(n+1)$	is the amount of heat passing from tube wall to phase interface;
$q_2 = G_l c_l(t_{out} - t_{in}) - q_1/n-1$	is the heat transferred from interface to solution;
$q_3 = n\lambda_s(t_{cr} - t_s)$	is the cooling of scale (t_s) by flow (the higher $n \approx < V'^2_{3e} >$ the lower the flow rate and the colder the flow);
$q_4 = L_{cr}\gamma_s \approx q_2\gamma_s$	is the heat content of scale;

$q_{wa} = G_{wa}\gamma_{wa}(t_{wa}-t_{cr}) = F_s(t_{st}-t_{cond})$ is the heat radiated by wall;
$b = n\lambda_s[(1/2) + (\delta_{wa}/\lambda_{wa})] = F_s n(t_{cond}-t_s)$.

LITERATURE CITED

1. R. D. Azelitskaya, N. A. Prikhodchenko, and V. F. Chernykh, in: Acoustic and Magnetic Treatments of Materials [in Russian], Novocherkassk (1966), p. 32.
2. A. A. Armand and E. I. Nevstrueva, Izv. Vses. Teplotekh. Inst., No. 2, 1 (1950).
3. Yu. P. Adler et al., Experiment Planning in Optimal-Condition Definition [in Russian], Nauka, Moscow (1971).
4. H. E. Buckley, Crystal Growth [Russian translation], Inostr. Lit., Moscow (1954).
5. R. Ya. Berlaga, Zap. Derzh. Fiz. Inst., No. 1, Ukrpoligraf (1930).
6. S. V. Bleshinskii, Izv. Akad. Nauk KirgSSR, No. 1, 65 (1968).
7. A. T. Bogorosh, I. M. Fedotkin, L. P. Zarudnev, and S. R. Bogorosh, in: The Food Industry [in Ukrainian], No. 1, Tekhnika, Kiev (1973).
8. Yu. T. Borshchevskii et al., in: Collections of Works of the Scientific and Technical Committee [in Russian], Izd. Khar' Kovsk. Politekh. Inst., No. 21, Khabarovsk (1970).
9. Yu. T. Borshchevskii and O. N. Lebedev, Tr. Novosibirsk. Inst. Inzh. Vodn. Transport, No. 26 (1967).
10. Yu. T. Borshchevskii, "Structure of the turbulence in a two-phase boundary layer," in: Proceedings of the International Conference on Reactor Coolants, London (1964).
11. Yu. T. Borshchevskii and N. A. Yakovlev, Izv. Sibirsk. Otd. Akad. Nauk SSSR, No. 10 (1963).
12. F. K. Gorskii and A. V. Akhromova, in: Liquid Crystallization [in Russian], No. 2, Minsk (1963), p. 3.
13. V. G. Inzhechek, Tr. Khar'kovsk. Inzh.-Ekon. Inst., No. 7, 43 (1956).
14. M. Iovchev, Yearbook of the Higher Institute of Heavy Electrical Engineering: Machine Design [in Bulgarian], No. 1, Izd. Tekhnika, Sofia (1967), p. 30.
15. A. N. Kirgintsev, V. M. Sokolov, and M. P. Burlakova, Izv. Sibirsk. Otd. Akad. Nauk SSSR, Khim., No. 1, 25 (1963).
16. A. N. Kirgintsev and V. M. Sokolov, Koll. Zh., 27, 697 (1965).
17. A. N. Kirgintsev and V. M. Sokolov, Zh. Prikl. Khim., 38, 1871 (1965).
18. A. N. Kirgintsev and V. M. Sokolov, Zh. Fiz. Khim., 40, 2053 (1966).
19. V. I. Klassen, in: New Physical and Physicochemical Slime Treatments in Mineral Dressing [in Russian], Nauka, Moscow (1967), p. 5.
20. V. F. Kovalenko, Tr. Tsentr. Nauchna-Issled. Inst. Morsk. Flota, No. 60 (1964).
21. Yu. M. Kostrikin, Izv. Vses. Teplotekh. Inst., No. 11 (1947).
22. V. V. Kondoguri, Zh. Russ. Fiz.-Khim. Obshch., Chast' Fiz., No. 8, 279 (1926).
23. V. D. Kuznetsov, Crystals and Crystallization [in Russian], Gostekhizdat, Moscow (1953).
24. N. N. Man'kina et al., in: Heat Engineering [in Russian], No. 2 (1959).
25. O. I. Martynova and E. F. Tebenikhin, Koll. Zh., 29, 692 (1967).
26. O. I. Martynova et al., Usp. Fiz. Nauk, 98, 195 (1969).
27. V. M. Minenko, Magnetic Treatment of Dispersed Water Systems [in Russian], Tekhnika, Kiev (1970).
28. G. L. Mikhnevich et al., Koll. Zh., 24, 491 (1962).
29. G. L. Mikhnevich et al., Koll Zh., 24, 488 (1962).
30. E. A. Nevstrueva et al., Inzh.-Fiz. Zh., 24, No. 1 (1973).
31. S. I. Pol'kin and A. I. Rafienko, Tsvetnye Metally, No. 9, 10 (1964).
32. M. Ya. Polyanskii, Tr. Leningradsk. Politekh. Inst., No. 2 (1953).
33. D. A. Rozenel', Water Treatment in Boilers and Stream-Engine Boiler Flushing [in Russian], Izd. Zap. Zhel. Dor., Vilnius (1947).
34. A. V. Smirnov, Author's Abstract of Candidate's Dissertation, Chernovtsy (1966).
35. M. A. Styrikovich, in: Physicochemical Processes in Boilers and the Water Conditions of High-Pressure Boilers [in Russian], Gosenergoizdat, Moscow (1951), p. 38-42.
36. E. F. Tebenikhin and B. T. Gusev, Magnetic Water Treatment in Heat Engineering [in Russian], Énergiya, Moscow (1970).
37. E. F. Tebenikhin and B. T. Gusev, Prom. Énergetika, 26, No. 11 (1963).
38. N. Yu. Tobilevich, I. I. Sagan', V. T. Garyazha, and A. A. Knyazev, in: The Food Industry [in Russian], No. 2, Tekhnika, Kiev (1965).
39. I. M. Fedotkin, Author's Abstract of Doctoral Dissertation, KTIPP, Kiev (1969).

40. I. M. Fedotkin, A. T. Bogorosh, N. I. Oseiko, and Yu. A. Kopylov, in: Transactions of the All-Union Scientific-Research and Experimental-Design Institute of Food Machinery [in Russian], No. 33, Moscow (1973).
41. I. M. Fedotkin and A. T. Bogorosh, in: The Food Industry [in Russian], No. 3, Tekhnika, Kiev (1965).
42. E. V. Khamskii, Crystallization from Solution [in Russian], Nauka, Leningrad (1967).
43. K. G. Shipov, Tr. Volgogradsk. Moloch. Inst., No. 9, 21 (1948).
44. R. Bianicci, Termotechnika, 16, No. 8 (1962).
45. H. Hiller, "Scale formation in sea-water distilling plants and its prevention," in: Proceedings of the Institute of Mechanical Engineers (JB), No. 7, London (1952).
46. R. S. Hall, Trans. ASME, 66, No. 5, 458 (1944).
47. E. R. Patridge and H. H. White, Amer. Soc. of Mech. Eng. (ASME), Rochester Melting (1929).
48. R. G. Peaver, "Distillation for marine purposes," Trans. Inst. Marine Eng., 72, No. 9, 339-362 (1960).